$$n = 4 \quad a_0 = 8.81 \times 10^{-12} \quad a_1 = -4.92 \times 10^{-13} \quad a_2 = 3.54 \times 10^{-14} \quad a_3 = -1.08 \times 10^{-15} \quad a_4 = 1.05 \times 10^{-17}$$

etc.

It is clear that it is not necessary to take a very long development. The practical devices have generally a geometry such as $w/h \geq 1$, so it is not necessary to give a fourth-order development for p because in the third-order one the ratio $|a_3/a_2|$ is very small ($\sim 2 \times 10^{-2}$). But if w/h is very small ($w/h < 0.1$), it would be necessary to take a larger n.

Figs. 4 and 5 give the graphs of the developments of p and the positions of the computed points. We can see on these graphs that a fourth-order development is sufficient to give a good representation of the variation of p with w/h.

Finally, we have the capacitance of a single microstrip line in terms of ϵ_r, w/h, and C_0. C_0 is the capacitance of the line without dielectric substrate. By a conformal mapping method [6], it is possible to calculate this last capacitance only in terms of ϵ_0 and w/h. Then the final result is that we have a formula giving the capacitances for all the possible configurations.

The same result can be obtained for the coupled line. We are currently working on this problem.

These results are very important, because they make very lengthy and expensive computations unnecessary in order to obtain impedance for the microstrip line, coupling coefficient, and adaptation for couplers and also phase displacement and group delay for meander lines.

REFERENCES

[1] R. Daumas, D. Pompei, E. Rivier, and A. Ros, "Extension de la théorie de Kirchoff aux lignes rubans couplées. Application au calcul des coupleurs en lignes à bandes," *Annal. Télécommun.*, vol. 28, pp. 325–334, 1973.

[2] T. G. Bryant and J. A. Weiss, "Parameters of microstrip transmission lines and of coupled pairs of microstrip lines," *IEEE Trans. Microwave Theory Tech. (1968 Symp. Issue)*, vol. MTT-16, pp.1021–1027, Dec. 1968.

[3] E. Yamashita and R. Mittra, "Variational method for the analysis of microstrip lines," *IEEE Trans. Microwave Theory Tech.*, vol. MTT-16, pp. 251–256, Apr. 1968.

[4] H.E. Green, "The numerical solution of some important transmission-line problem," *IEEE Trans. Microwave Theory Tech. (Special Issue on Microwave Filters)*, vol. MTT-13, pp. 676–692, Sept. 1965.

[5] R. Daumas, D. Pompei, E. Rivier, and A. Ros, "Faster impedance estimation for coupled microstrips with an overrelaxation method," *IEEE Trans. Microwave Theory Tech.* (Short Papers), vol. MTT-21, pp. 552–556, Aug. 1973.

[6] H. A. Wheeler, "Transmission-line properties of parallel wide strips by a conformal mapping approximation," *IEEE Trans. Microwave Theory Tech.*, vol. MTT-12, pp. 280–289, May 1964.

Inductance of Nonstraight Conductors Close to a Ground Return Plane

A. E. RUEHLI, SENIOR MEMBER, IEEE, N. KULASZA, AND J. PIVNICHNY, SENIOR MEMBER, IEEE

***Abstract*—Measurement and calculation of the inductance of a nonstraight conductor close to ground return plane are considered. An equivalent circuit model solution is given, and the results are compared to measurements for a corner-type geometry. Much larger changes in inductance as a function of frequency have been observed for the corner-type geometry than for the equivalent straight-conductor geometry. The circuit model can be used to predict the inductance for other configurations.**

Manuscript received August 16, 1974; revised April 4, 1975.

A. E. Ruehli is with the IBM Thomas J. Watson Research Center, Yorktown Heights, N. Y. 10598.

N. Kulasza and J. Pivnichny are with IBM Endicott, Endicott, N. Y. 13760.

I. INTRODUCTION

Although strip-type transmission lines are considered to be mostly two-dimensional, they often have corner-type discontinuities. Typical examples are wires in ceramic digital circuit packages [1] or stripline filter applications [2]. Two cases can be distinguished depending on whether ground planes are close to the wires or are remote (or entirely absent). A three-dimensional formulation based on a low-frequency approximation [3] leads to rather accurate inductance values for wires without nearby ground planes. Essentially, the current redistribution with frequency, usually called skin effect, leads to only a small variation in inductance. Two changes take place in inductance for wires close to a ground return plane for the L-shaped geometry shown in Fig. 1. A relatively small inductance variation is associated with the redistribution of current in the strip conductor [4] while, as shown here, a very large change in inductance can be associated with the redistribution of current in the ground plane. For high frequencies, the current will flow under the strip conductor since this provides a low-inductance path. At lower frequencies, current will flow across the ground plane due to the lower resistance and larger inductance associated with this path. The onset of the two changes in inductance depends on the relative conductance and thickness of the strip conductor compared to the ground plane. The model used in [4], where a perfect image is assumed, may be sufficient at microwave frequencies for a strip conductor close to a highly conductive substrate. The ground-plane effect discussed here is more important for time-domain applications where the pulses contain a large spectrum of frequencies, as well as for low-conductance substrates like semiconductor chips.

Another important aspect associated with the L-shaped conductor geometry to be considered is the high-frequency discontinuity inductance which is reported elsewhere [5], [6]. Thus the work presented in this short paper, when used in conjunction with that referenced previously, leads to a characterization of the L-shaped conductor geometry for a wide range of frequencies.

In Section II, a partial-element equivalent circuit (PEEC) model [7] will be presented, while a comparison between the computer model and measurements will be given in Section III.

II. PARTIAL-ELEMENT EQUIVALENT CIRCUIT MODEL

The reader is referred to [7] for details concerning the PEEC model employed. Simple considerations show that the capacitances can be ignored for the physical structure analyzed here over the frequency range of interest. The equivalent circuit is based on the cells into which the structure is divided as shown in Fig. 2. The nodes indicated coincide with the nodes in the circuit model. The equivalent circuit corresponding to the numbered nodes in Fig. 2 is given in Fig. 3, and only the elements in the X direction are labeled. Note that this is only a small portion of the rather complex circuit. The construction of the total circuit should, however, be evident. Coupling exists among all the partial inductances corresponding to current in the same direction, while all inductances with cell currents perpendicular to one another are decoupled. The

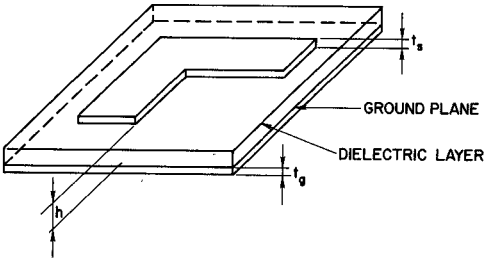

Fig. 1. L-shaped strip conductor on thin ground plane.

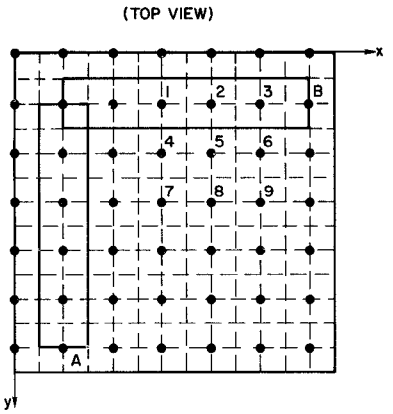

Fig. 2. Cell geometry for L-shaped conductor.

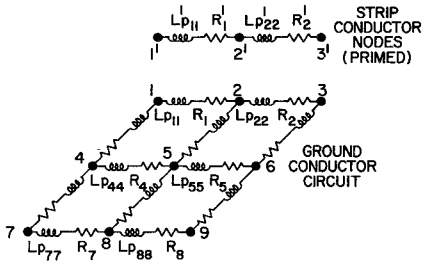

Fig. 3. Portion of equivalent circuit for cells numbered in Fig. 2.

number of partial inductances which are evaluated with the inductance formulation in [3] is very small due to the symmetry of the problem and since coupling is restricted to cells which are close to each other. Fig. 4 illustrates the neighboring cells of interest for the inductance computation, while the inductance values are given in Table I. For the model which is restricted to single neighbor coupling only, the cells 1 for the ground and strip are assumed to couple only to cells 2, 4, and 5. The mutual coupling from cell 1 to cells 3, 6, 7, 8, and 9 is included additionally in the model which couples over two cells. It is noted that mutual coupling over one or two cells is also accounted for in the strip conductor as is indicated in Table I. The strip conductor is represented by cells having the full conductor width, and thus the current is assumed to be uniform over the entire width. Mainly, it is shown in [4] that the inductance variation due to the current redistribution in the strip conductor (and its perfect image) is small compared to the change due to the ground conductor. Almost the same size cells have been chosen for both strip and ground conductor which leads to a simplification of the PEEC. The strip width is 12.7 mm and the spacing is $h = 0.127$ mm.

The PEEC model is entered in a circuit analysis program like ASTAP [8], [9]. The model constructed here has 197 nodes and 707 input statements for the program to describe the circuit elements for coupling over neighboring cells only. The model with coupling over two neighboring cells contains 1375 input statements where the increase is due to the added mutual partial inductances.

III. RESULTS AND COMPARISON

In both the measurement and the computer model, point B is a connection between ground and the top conductor, while the impedance is measured at point A. The model impedance is evaluated by using the ASTAP [8], [9] computer program. In essence, a unit current is impressed at point A, and the complex voltage computed between ground and point A is $R(f) + j\omega L(f)$. For the measurement, the bridge is connected at point A with a miniature coaxial cable perpendicular through the ground plane to avoid coupling [3]. Comparing the two models for coupling over one and two neighboring cells, it is noted that the difference in the computed impedance in Fig. 5 is not significant, especially when one considers that the

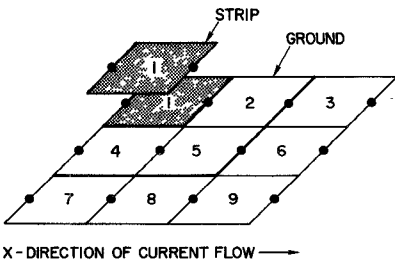

Fig. 4. Cells for inductances in horizontal direction.

TABLE I
PARTIAL INDUCTANCES CORRESPONDING TO FIG. 4

Cell to Cell Inductances				
	L(nH)	Strip to Strip Cells	Strip to Ground Cells	Ground to Ground Cells
Same position	L_{p11}	5.57	5.01	4.91
Nearest Neighbors	L_{p12}	1.92	1.87	1.84
	L_{p14}	-	1.75	1.83
	L_{p15}	-	1.23	1.24
Two positions away	L_{p13}	0.851	0.847	0.843
	L_{p16}	-	0.753	0.752
	L_{p17}	-	0.836	0.843
	L_{p18}	-	0.748	0.752
	L_{p19}	-	0.59	0.59

Cell data: Ground Cell:
Size (mm): $16.51^2 \times 0.0356$
Resistance (mΩ): 0.485
Strip Cell:
Size (mm): $16.51 \times 12.7 \times 0.0356$
Resistance (mΩ): 0.63

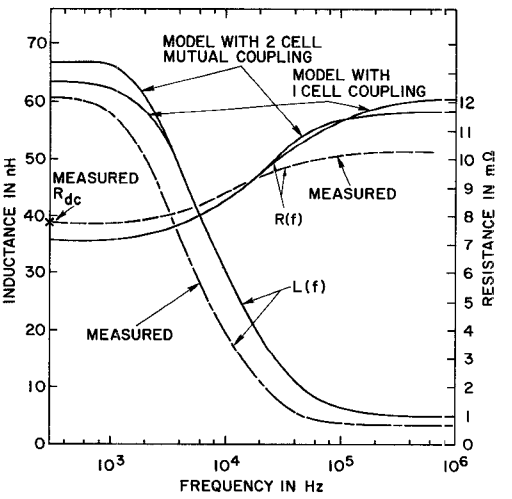

Fig. 5. Comparison between model and measurement.

model with coupling over two cells requires almost twice as many input language statements for the circuit description. Further, the error due to the rather large cell size is the same in both models. The measured curve in Fig. 5 shows that the model predicts the measured impedance rather well. Since the accurate measurement of the low-impedance loop is difficult, three values have been averaged at each frequency point to improve confidence. Preliminary measurements on the same geometry with another conductor added, such that a U-shaped strip conductor results, showed an even larger inductance variation with frequency.

IV. CONCLUSIONS

The equivalent circuit model which has been presented is capable of predicting the inductance of nonstraight conductors as a function of frequency. When applied to corner-type geometries, the inductance was found to be much larger than for straight conductors assuming that both are close to a ground plane.

ACKNOWLEDGMENT

The authors wish to thank H. Lord who contributed to the project in its initial stages. Also, the helpful discussions with P. Grau are acknowledged.

REFERENCES

[1] R. W. Ilgenfritz, L. E. Mogey, and D. W. Walter, "A high density thick film multilayer process for LSI circuits," *IEEE Trans. Parts, Hybrids Packag.*, vol. PHP-10, pp. 165–168, Sept. 1974.
[2] V. A. Monaco and P. Tiberio, "Computer-aided analysis of microwave circuits," *IEEE Trans. Microwave Theory Tech. (Special Issue on Computer-Oriented Microwave Practices)*, vol. MTT-22, pp. 249–263, Mar. 1974.
[3] A. E. Ruehli, "Inductance calculations in a complex integrated circuit environment," *IBM J. Res. Develop.*, vol. 16, pp. 470–481, Sept. 1972.
[4] A. Gopinath and P. Silvester, "Calculation of inductance of finite-length strips and its variation with frequency," *IEEE Trans. Microwave Theory Tech.*, vol. MTT-21, pp. 380–386, June 1973.
[5] A. Gopinath and B. Easter, "Moment method of calculating discontinuity inductance of microstrip right-angled bends," *IEEE Trans. Microwave Theory Tech.* (Short Papers), vol. MTT-22, pp. 880–883, Oct. 1974.
[6] A. F. Thomson and A. Gopinath, "Calculation of microstrip discontinuity inductances," this issue, pp. 648–655.
[7] A. E. Ruehli, "Equivalent circuit models for three-dimensional multiconductor systems," *IEEE Trans. Microwave Theory Tech. (Special Issue on Computer-Oriented Microwave Practices)*, vol. MTT-22, pp. 216–221, Mar. 1974.
[8] W. T. Weeks *et al.*, "Algorithms for ASTAP—A network analysis program," *IEEE Trans. Circuit Theory (Special Issue on Computer-Aided Design)*, vol. CT-20, pp. 628–634, Nov. 1973.
[9] IBM Advanced Statistical Analysis Program, ASTAP Manual SH20-1118-0.

Prototype Characteristics for a Class of Dual-Mode Filters

ROBERT D. WANSELOW, SENIOR MEMBER, IEEE

***Abstract*—Selected prototype characteristics of nonequiripple antimetric elliptic-function filters which can be realized in orthogonal cascaded dual-mode circular or square waveguide structures are presented. Cavity-coupling data for 4-, 6-, and 8-section 0.01- and 0.05-dB-ripple passband designs with variable stopband levels are tabulated. Quantitative comparisons of elliptic and Chebyshev filter designs are also discussed, indicating the superior characteristics of elliptic networks.**

Manuscript September 26, 1974; revised February 24, 1975.
The author is with the TRW Systems Group, Redondo Beach, Calif. 90278.

INTRODUCTION

In recent years considerable emphasis has been placed on optimizing not only the electrical, but also the mechanical characteristics of narrow-band microwave communications waveguide bandpass filters. Near-optimum amplitude characteristics can be achieved utilizing elliptic functions which exhibit amplitude ripple in both the passband and stopbands [1]. However, the microwave realization of these near-optimum polynomials in the form of coupled cavities requires a departure from conventional cascaded synchronously tuned resonators [2] which exhibit a monotonically increasing stopband attenuation with or without a passband ripple response. That is, negative coupling must be available between predetermined sets of cavities. To achieve this, the hardware realization of such networks may make use of degenerate dual modes in single waveguide cavities, an idea which was first proposed by Ragan [3]. An added feature of the dual-mode cavity is the obvious reduction in size and weight.

In several excellent papers by Atia and Williams [4]–[7] the theory, together with experimental verification of various types of elliptic filters employing negative coupling in waveguide structures, has been well documented. The objective of this short paper is to present selected prototype parametric characteristics of antimetric elliptic-function filters which can be transformed into bandpass networks with emphasis directed toward cascaded dual-mode waveguide structures. Extensive tables of resonator coupling data for 4-, 6-, and 8-section filters have been developed as an aid for rapid design of these networks. All tabular data presented were generated from computer programs.

PROTOTYPE NETWORK CHARACTERISTICS

The equivalent circuit for N coupled cavities is shown in Fig. 1 which, for dual-mode operation, may include the additional terminal cross couplings indicated (M_{14} and $M_{N-3,N}$) and the M_{ij} coupling which exists for $N \geq 8$ sections, i.e., $M_{ij} = M_{36}$, where $(N = 8)$. Fig. 2 denotes the general orthogonal TE_{0n}-mode circular

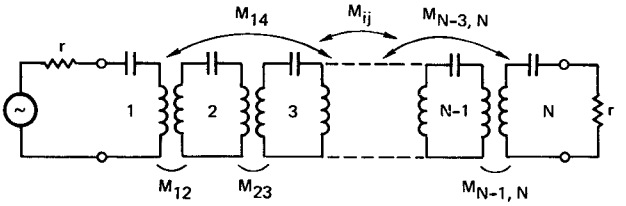

Fig. 1. Equivalent circuit of N coupled cavities (N = 4–8). Cross couplings available: $N = 4$: M_{14}; $N = 6$: $M_{14} = M_{36}$; $N = 8$: $M_{14} = M_{58}$, $M_{ij} = M_{36}$.

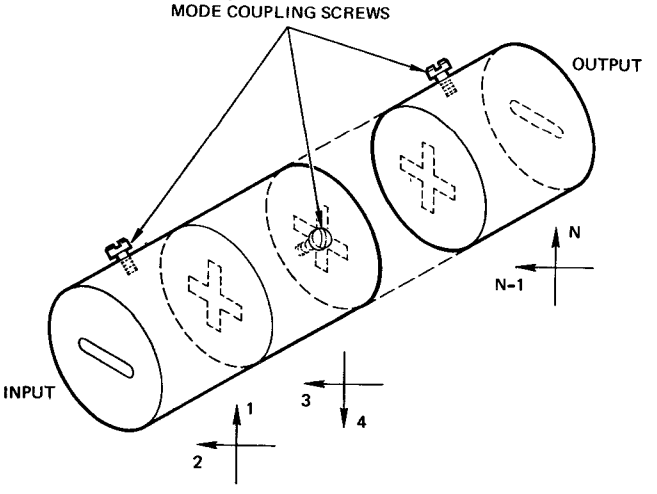

Fig. 2. Cascaded dual-mode circular-waveguide-cavity filter.